Research Journal of Biological Sciences 4 (11): 1156-1161, 2009
ISSN: 1815-8846

Antibacterial Activity of Silver/Clay/Chitosan Bionanocomposites

[1]Mansor Bin Ahmad, [1]Kamyar Shameli, [2]Majid Darroudi, [1]Wan Md Zin Wan Yunus,
[1]Nor Azowa Ibrahim, [3]Azizah Abdul Hamid and [3]Mohsen Zargar
[1]Department of Chemistry, Faculty of Science, University Putra Malaysia,
43400 UPM Serdang, Selangor, Malaysia
[2]Advanced Materials and Nanotechnology Laboratory, Institute of Advanced Technology (ITMA),
University Putra Malaysia, 43400 UPM Serdang, Selangor, Malaysia
[3]Department of Food Science, Faculty of Food Science and Biotechnology,
Putra Malaysia University, 43400 Serdang, Selangor, Malaysia

Abstract: A simple synthesis of silver/montmorillonite/chitosan (Ag/MMT/Cts) Bionanocomposites (BNCs) with controllable sizes is presented. In this research, reduction process of silver cations by UV-irradiation was performed. $AgNO_3$, MMT and chitosan were used as a silver precursor, solid support and stabilizer, respectively. The properties of Ag/MMT/Cts BNCs were studied as a function of UV-irradiation time. We found that UV-irradiation disintegrated the silver nanoparticles (Ag-NPs) into smaller size until a relatively stable size and size distribution were achieved. The average size, size distribution and crystalline structure of Ag-NPs were determined by Transmission Electron Microscopy (TEM) and Powder X-Ray Diffraction (PXRD). The antibacterial activity of Ag-NPs was investigated against Gram-negative bacterium (*Escherichia coli* (*E. coli*)) and Gram-positive bacteria (*Staphylococcus aureus* (*S. aureus*) and Methicillin-Resistant *Staphylococcus Aureus* (MRSA)) by disk diffusion method using Muller-Hinton Agar (MHA) at different sizes of Ag-NPs. All of synthesized Ag/MMT/Cts BNCs were found to have high antibacterial activity. These results showed that Ag/MMT/Cts BNCs can be useful in different biological research and biomedical applications such as surgical devices and drug delivery vehicles.

Key words: Antibacterial activity, silver nanoparticles, bionanocomposites, montmorillonite, chitosan, UV-irradiation

INTRODUCTION

The synthesis of nanomaterials with the desired quality is one of the most exciting aspects in modern nanoscience and nanotechnology (Bhattacharya and Gupta, 2005). Among metal nanoparticles, silver nanoparticles (Ag-NPs) have been known to have inhibitory and antibacterial properties (Cho *et al*., 2005). The Ag-NPs interactions with bacteria are dependent on the size and shape of the nanoparticles but bactericide mechanism of Ag-NPs is not clear (Morones *et al*., 2005; Pal *et al*., 2007). The antibacterial activity of the Ag-NPs can be used in several biomedical applications, for example, to reduce infections in burn treatment (Ulkur *et al*., 2005) and human skin (Bosetti *et al*., 2002; Gauger *et al*., 2003).

MMT as lamellar clay has intercalation, swelling and ion exchange properties. Its interlayer space has been used for the synthesis of nanoparticles materials and biomaterials, as support for anchoring transition-metal complex catalysts and as adsorbents for cationic ions (Kozak and Domka, 2004).

In this research, the effect of Ag-NPs size on antibacterial property is presented. In addition, the antibacterial activity of Ag^+ was investigated and compared with antibacterial activity of prepared Ag-NPs. Via this method, we are able to obtain Ag-NPs with different sizes and antibacterial activity by controlling the UV-irradiation time. Similar studies on Ag-NPs prepared by chemical and physical reduction methods have been reported (Abdullah *et al*., 2009; Hamid *et al*., 2009).

MATERIALS AND METHODS

All reagents were of analytical grades and were used as received without further purification. $AgNO_3$ (99.98%) used as silver precursor was supplied from Merck, Germany. MMT, used as a solid support for Ag-NPs, was

Corresponding Author: Mansor Bin Ahmad, Department of Chemistry, Faculty of Science, University Putra Malaysia, 43400 UPM Serdang, Selangor, Malaysia

purchased from Kunipa-F, Japan. Chitosan (Low molecular weight, Sigma-Aldrich, USA) was used as a stabilizer agent. Glacial acetic acid (HAC, 99%), as a solvent for chitosan, was purchased from Sigma-Aldrich, USA. All aqueous solutions were prepared with double distilled water (DD-water).

Synthesis of Ag/MMT/Cts BNCs: Chitosan sol (100 mL, 2.0% wt.) were prepared by solubilizing chitosan in 1.0% wt. of HAC sol (pH~3.45) under constant stirring for 1 h. Five hundred milliliter of $AgNO_3$ (0.02 M) was added into the chitosan sol under constant stirring for preparation of $Cts/AgNO_3$ sol. For preparation of MMT suspension, 5.0 g of MMT was dispersed in 400 mL DD water and was vigorously stirred for 1 h. The $Cts/AgNO_3$ was added into the MMT suspension and the mixture was further vigorously stirred for 4 h at the room temperature to obtained $MMT/Cts/AgNO_3$ sol. The $MMT/Cts/AgNO_3$ sol. was irradiated using the UV reactor with UV-lamp at λ = 365 nm, while it was stirred at speed of 195 rpm. The irradiation times of 0 h (S0), 1 h (S1), 3 h (S2), 18 h (S3), 48 h (S4) and 96 h (S5) were applied for different cuvettes, respectively. Then, obtained suspensions of Ag/MMT/Cts BNCs were centrifuged, washed with DD-water twice and dried at 40°C under vacuum overnight. All experiments were conducted at ambient temperature.

Evolution of antibacterial activity: *In vitro* antibacterial activity of the samples was evaluated by disc diffusion method using Mueller-Hinton Agar (MHA) with determination of inhibition zones in millimeter (mm), which conforms to the recommended standards of the National Committee for Clinical Laboratory Standards (NCCLS). *Escherichia coli* (ATCC 25922), *Staphylococcus aureus* (ATCC 25923) and Methicillin-Resistant *Staphylococcus aureus* (MRSA) (ATCC 700689) were used for antibacterial effect assay. Briefly, sterile paper discs (6 mm) impregnated with 20 μL of Ag/MMT/Cts BNCs (S2, S4 and S5) with different treatment times suspended in sterile distilled water and were left to dry in 37°C for 24 h in sterile condition. Bacterial suspension prepared by making a saline suspension of isolated colonies selected from an 18-24 h tryptic soy agar plate. The suspension was adjusted to match the tube 0.5 McFarland turbidity standard using spectrophotometer in 600 nm, which equal to 1.5×10^8 Colony-Forming Units (CFU mL^{-1}).

The surface of MHA was completely inoculated using sterile swab which steeped in prepared suspension of bacterium. Finally, impregnated discs were placed on the inoculated agar and the petri dish was incubated at 37°C for 24 h. After incubation the diameter of growth inhibition zones were measured. Chloramphenicol (30 μg) and Cefotaxime (30 μg) were used as positive standards in order to control the sensitivity of the bacteria. All tests were done in triplicate.

Characterization: The Ag/MMT/Cts BNCs were characterized using ultraviolet-visible (UV-vis) spectroscopy, Transmission Electron Microscopy (TEM) and Powder X-Ray Diffraction (PXRD). The UV-vis spectra were recorded over the range of 300-700 nm with (H.UV.1650 PC, SHIMADZU) UV-vis spectrophotometer. Transmission Electron Microscopy (TEM) observations were carried out on A Hitachi H-7100 electron microscope and the particle size distributions were determined using the UTHSCSA Image Tool version 3.00 program. The structure of Ag/MMT/Cts BNCs has been studied using powder X-ray diffraction (PXRD-6000 SHIMADZU). The change in interlamellar spacing of MMT and Ag/MMT/Cts BNCs was also studied by PXRD in the angle range of $2°<2\theta<12°$. The PXRD patterns were recorded at a scan speed of 2°C min^{-1}. The reactions were carried out on a UV reactor (UV-A, 6W).

RESULTS AND DISCUSSION

The colour of prepared samples at different UV-irradiation times gradually changed from colourless to light gray then to gray and finally to dark gray, indicating the formation of Ag-NPs in MMT/Cts suspension. When the $MMT/Cts/AgNO_3$ suspension was irradiated under UV for 3 h (S2), photo-reduced Ag-NPs were formed with a broad size distribution and mean diameter of about 4.60±1.31 nm (Fig. 1a and b). As it can be seen from (Fig. 1c and d), when the irradiation time was increased in S4, the mean diameter of Ag-NPs decreased considerably to 3.16±0.95 nm as compared to S2. It can be seen that larger Ag-NPs were obtained under shorter irradiation time and they disintegrated under the further UV-irradiation (Huang and Yang, 2008).

Figure 1e and f show no large decrease in the particle size and change in size distribution can be observed in S5 (2.72±0.53 nm), when compared with S4. This indicates that the Ag-NPs obtained in this irradiation time are extremely stable.

As shown in Fig. 2, the original d_L of MMT, 1.24 nm and in MMT/Cts is increased to1.67 nm at smaller 2θ angles (2θ = 7.12° for MMT and 2θ = 5.26° for MMT/Cts) by chitosan intercalation. The d_L in S5 also was increase to 1.70 nm at smaller 2θ angles (2θ = 5.16°) by silver intercalation. Theses d_L values are direct proof of intercalation structures. Metallic nanoparticles formed at the latter location are the cause of the increase in basal spacing. In these samples the intensities of the reflections

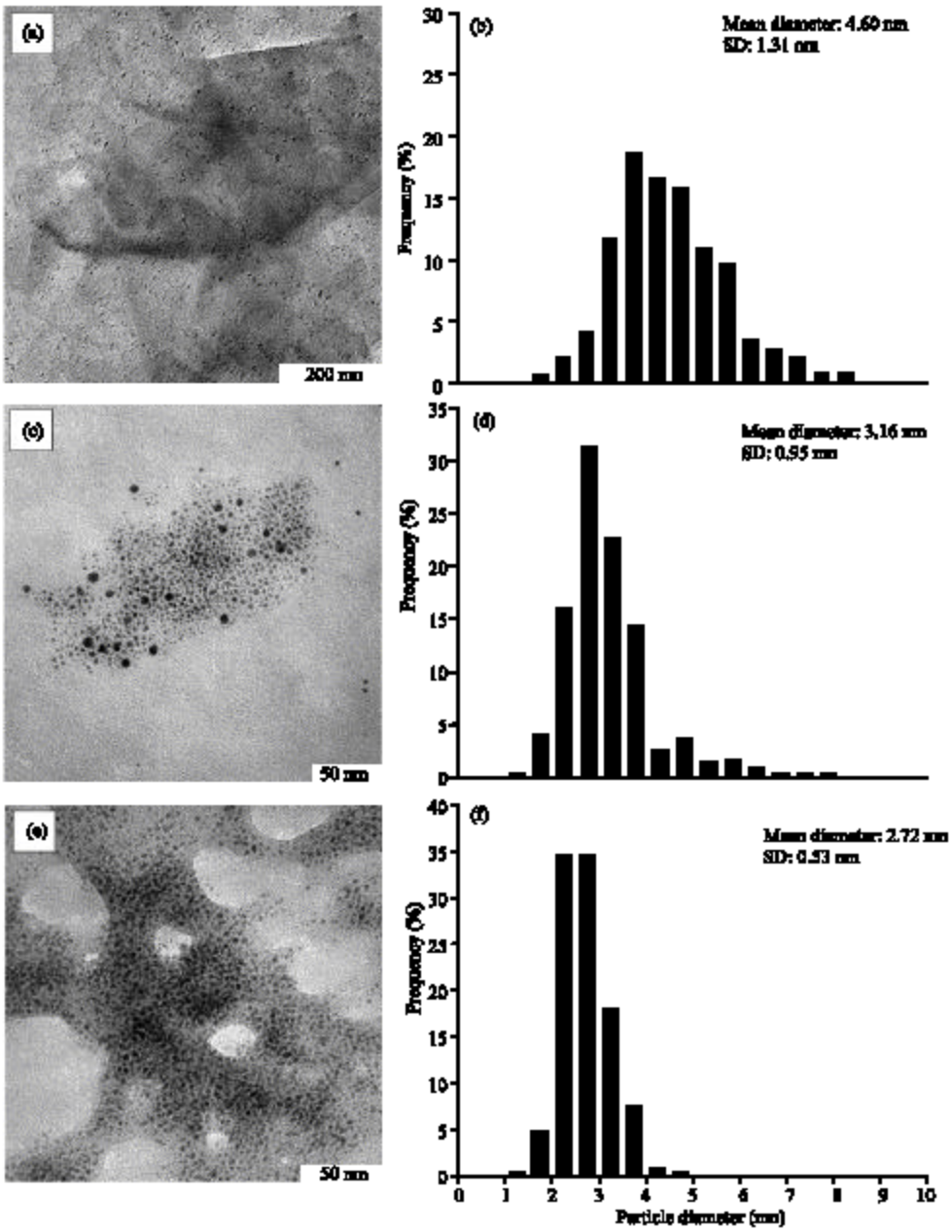

Fig. 1: TEM images and their corresponding particle size distributions of Ag-NPs at different UV-irradiation times; S2 (a and b), S4 (c and d) and S5 (e and f)

are significantly lower whereas their half-widths are larger than those of undoped clay minerals: the highly ordered parallel lamellar structure of the mineral is disrupted by particle formation (Patakfalvi *et al*., 2003).

The PXRD peaks at 2θ of 38.07°, 44.23°, 64.52° and 77.30° (Fig. 3) can be attributed to the 111, 200, 220 and 311 crystallographic planes of face-centered cubic (fcc) silver crystals, respectively (Temgire and Joshi, 2004). The PXRD peak broadenings of Ag-NPs are mostly because of existing of nano-sized particles (Prasad *et al*., 2006). In addition there is a characteristic peak at about 2θ = 62.5° that related to MMT clay (PXRD Ref. No. 00-003-0010) as a stable substrate.

The characteristic silver Surface Plasmon Resonance (SPR) band was detected around 330 nm (Fig. 4), when the UV-irradiation duration exceeded 3 h. For S3 and S4 the absorbance was observed at 331 nm and its intensity obviously has increased compared to S2. The increase

of the absorbance with further UV-Irradiation time indicates that the concentration of Ag-NPs increases (Bohren and Huffman, 1998) because the photo-induced fragmentation of Ag-NPs has increased the total number of particles in the solution. For S5, the absorbance increased considerably and was red-shifted to 336 nm.

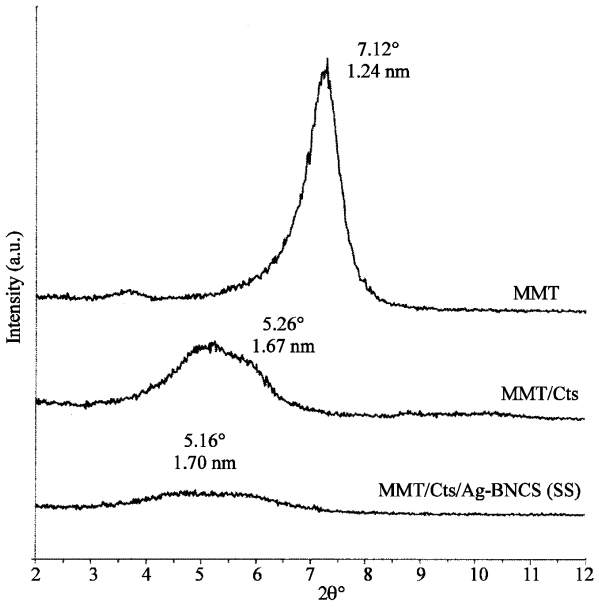

Fig. 2: PXRD patterns of MMT and Ag/MMT/Cts BNCs (S5) for determination of d-spacing (d_L)

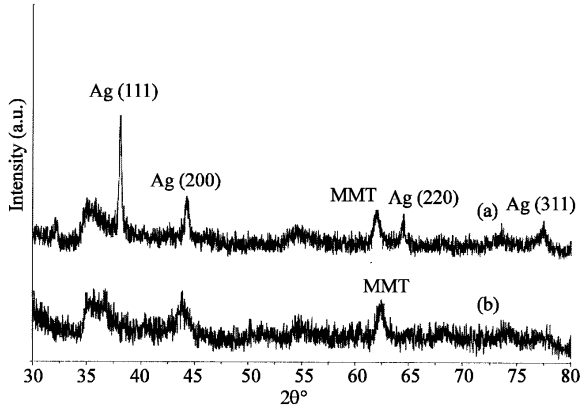

Fig. 3: PXRD patterns of; a) Ag/MMT/Cts BNCs (S5) and b) MMT

This is consistent with earlier findings that at higher concentration of metal nanoparticles may also lead to the red-shift of SPR band (Liu *et al*., 1998).

Inhibition zones values were obtained for the synthesized nanoparticles tested against *E. coli*, *S. aureus* and MRSA. The results and images of inhibition zones are presented as average values in Table 1 and Fig. 5, respectively.

Table 1 shows that the Ag-NPs give high and similar antibacterial activity against Gram-positive bacteria and Gram-negative bacterium. Because of their size, Ag-NPs can easily reach the nuclear content of bacteria and they present the greatest surface area; therefore the contact with bacteria is the greatest (Lok *et al*., 2006).

The Ag/MMT/Cts BNCs sols were used in the form in which they had been prepared. Therefore, antibacterial tests of solutions containing the reaction components were performed.

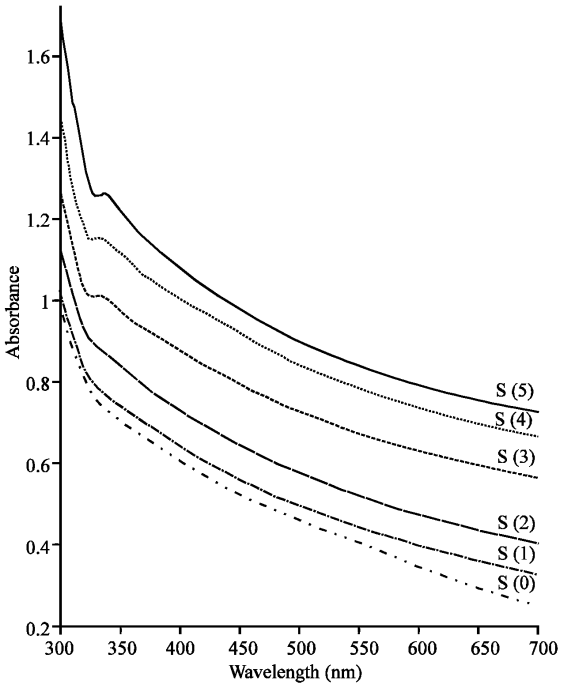

Fig. 4: UV-vis absorption spectra of Ag/MMT/Cts BNCs at different UV-irradiation times

Table 1: Average of inhibition zones for synthesized Ag/MMT/Cts BNCs

	Inhibition zone (mm)						
					Control negative (mm)	Control positive (mm)	
Bacteria	S0	S2	S4	S5	MMT	Cefotaxime	Chloramphenicol
E. coli	8.5	9.0	9.0	9.0	NA*	23	18
S. aureus	9.5	9.5	9.5	9.5	NA	25	19
MRAS	8.5	8.5	8.5	8.5	NA	20	17

*Not appear

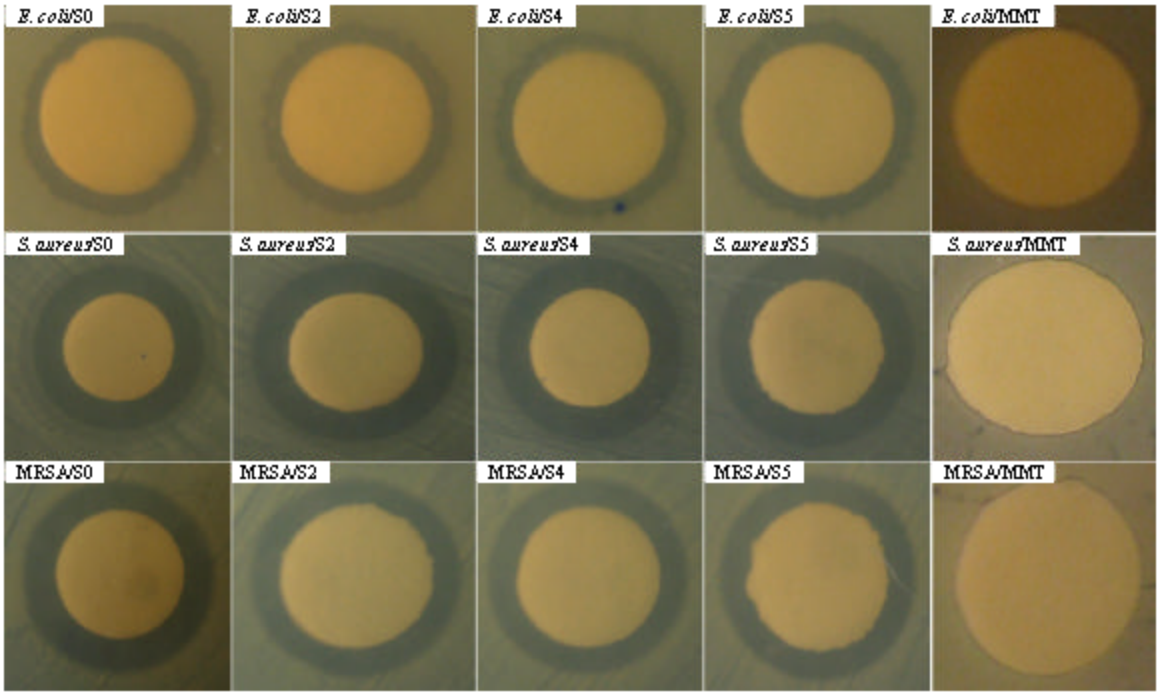

Fig. 5: The image of antibacterial activities of prepared samples against different bacteria

CONCLUSION

In this study, Ag/MMT/Cts BNCs with different sizes of Ag-NPs were synthesized in interlayer of MMT in an aqueous solution by UV-irradiation method and characterized using TEM, PXRD and UV-vis absorption spectroscopy. The antibacterial properties of these nanoparticles to different bacteria (Gram-positive and Gram-negative) including multiresistant strains were successfully demonstrated.

REFERENCES

Abdullah, A.H., A.A. Hamid, K. Shameli, M. Darroudi, M.B. Ahmad, M. Zargar and N.A. Ibrahim, 2009. Antibacterial effect of synthesized silver/montmorillonite nanocomposites by UV-Irradiation method. Res. Biol. Sci., 4: 1056-1060.

Bhattacharya, D. and R.K. Gupta, 2005. Nanotechnology and potential of microorganisms. Crit. Rev. Biotechnol., 25: 199-204.

Bohren, C.F. and D.R. Huffman, 1998. Absorption and Scattering of Light by Small Particles. Wiley Interscience, New York, pp: 544.

Bosetti, M., A. Masse, E. Tobin and M. Cannas, 2002. Silver coated materials for external fixation devices: *In vitro* biocompatibility and genotoxicity. Biomaterials, 23: 887-892.

Cho, K.H., J.E. Park, T. Osaka and S.G. Park, 2005. The study of antimicrobial activity and preservative effects of nanosilver in gradient. Electrochim. Acta, 51: 956-960.

Gauger, A., M. Mempel, A. Schekatz, T. Schafer, J. Ring and D. Abeck, 2003. Silver-coated textiles reduce *Staphylococcus aureus* colonization in patients with atopic eczema. Dermatology, 207: 15-21.

Hamid, A.A., K. Shameli, M. Darroudi, M.B. Ahmad, M. Zargar, N.A. Ibrahim and W.Z.W. Yunus, 2009. Synthesis and antibacterial activity of silver/montmorillonite nanocomposites. Res. Biol. Sci., 4: 1032-1036.

Huang, H. and Y. Yang, 2008. Preparation of silver nanoparticles in inorganic clay suspensions. Comp. Sci. Technol., 68: 2948-2953.

Kozak, M. and L.J. Domka, 2004. Adsorption of the quaternary ammonium salts on montmorillonite. J. Phys. Chem. Solids, 65: 441-445.

Liu, Z., H. Wang, H. Li and X. Wang, 1998. Red shift of plasmon resonance frequency due to the interacting Ag nanoparticles embedded in single crystal SiO_2 by implantation. Applied Phys. Lett., 72: 1823-1825.

Lok, C.M., C.M. Ho, R. Chen, Q.Y. He and W.Y. Yu *et al*., 2006. Proteomic analysis of the mode of antibacterial action of silver nanoparticles. J. Proteome Res., 5: 916-924.

Morones, J.R., J.L. Elechiguerra, A. Camacho, K. Holt, J.B. Kouri, J.T. Ramirez and M.J. Yacaman, 2005. The bactericidal effect of silver nanoparticles. Nanotechnology, 16: 2346-2353.

Pal, S., Y.K. Tak and J.M. Song, 2007. Does the antibacterial activity of silver nanoparticles depend on the shape of the nanoparticle? A study of the Gram-negative bacterium *Escherichia coli*. Applied Environ. Microbiol., 73: 1712-1720.

Patakfalvi, R., A. Oszko and I. Dekany, 2003. Synthesis and characterization of silver nanoparticle/kaolinite composites. Colloids Surfaces A: Physicochem. Eng. Aspects, 220: 45-54.

Prasad, V., C.D. Souza, D. Yadav, A.J. Shaikh and N. Vigneshwaran, 2006. Spectroscopic characterization of zinc oxide nanorods synthesized by solid-state reaction. Spectrochim. Acta Part A: Mol. Biomol. Spectroscopy, 65: 173-178.

Temgire, M.K. and S.S. Joshi, 2004. Optical and structural studies of silver nanoparticles. Radiat. Phys. Chem., 71: 1039-1044.

Ulkur, E., O. Oncul, H. Karagoz, E. Yeniz and B. Celikoz, 2005. Comparison of silver-coated dressing (Acticoat™), chlorhexidine acetate 0.5% (Bactigrass) and fusidic acid 2% (Fucidin) for topical antibacterial effect in methicillin-resistant staphylococci contaminated, full-skin thickness rat burn wounds. Burns, 31: 874-877.